Integrated active mixing and biosensing using low frequency vibrating mixer and Love-wave sensor for real time detection of antibody binding event

[1]F. Kardous, [2]L. El Fissi, [3]J-M Friedt, [1]F.Bastien, [1]W. Boireau, [1]R. Yahiaoui, [1]JF. Manceau, [1, 3]S. Ballandras

[1]Institut FEMTO-ST, Université de Franche-Comté, CNRS, ENSMM, UTBM F-25044 Besançon, France

[3] SENSeOR, Besançon, France

Emails: [1] faten.kardous@femto-st.fr, [2] lamia.elfissi@femto-st.fr, [3] jmfriedt@femto-st.fr

Telephone: (+33) 381402941

Fax: (+33) 381402809

Abstract:

Development of Lab-On-Chip devices is expected to dramatically change biochemical analyses, allowing notable increase of processing quality and throughput provided the induced chemical reactions are well controlled. In this work, we investigate the impact of local acoustic mixing to promote or accelerate such biochemical reactions, such as antibody grafting on activated surfaces.

During microarray building, the spotting mode leads to low efficiency in the ligand grafting and heterogeneities which limit its performances. To improve the transfer rate, we induce a hydrodynamic flow in the spotted droplet to disrupt the steady state during antibody grafting. To prove that acoustic mixing increases Antibody transfer rate to biochip surface, we have used a Love-wave sensor allowing for real-time monitoring of the biological reaction,

for different operation conditions (with or without mixing). An analysis of the impact of the proposed mixing on grafting kinetics is proposed and finally checked in the case antibody-antigen combination.

Keywords: Real-time biosensing; Acoustic mixer; Microarray; Ab immobilization;

1. Introduction

Although numerous work have been directed to the development of Lab-on-Chip devices for improving bio-chemical analysis, there is still a large interest in investigating new solutions for accurate detection and reaction monitoring, particularly using guided acoustic waves because of their remarkable sensitivity, and stability [1]-[3].

This study focuses on the analysis of biochemical reaction kinetics measured using direct detection biosensors. The two most common transducers in the field of direct detection biosensors are based on the conversion of an adsorbed mass to an electrical velocity through the interaction with an acoustic wave (quartz crystal resonators and surface acoustic wave sensors) [4]-[6], or with an evanescent electromagnetic wave (Surface Plasmon Resonance) [7]-[11]. Beyond the difference in the interaction mechanism, most of these devices allow for monitoring the adsorption kinetics as the solution stands still in an open well configuration, with some significant developments in the area of packaging towards continuous flow of the reagents which appears as a significant challenge for acoustic sensors [12-14]. One significant exception to this approach is Biacore's SPR system in which the reagents flow in a microfluidic channel [15, 16]. The SPR system is equipped with a microfluidic cartridge,

allowing for a dynamic circulation of fluid and so a dynamic transfer of biological molecules to a biochip surface. Nevertheless, in the case of low Reynolds number hydrodynamic flows, and particularly in the case of high Damkohler number, reactions with the active surface are mainly governed by diffusive effects [17]. Therefore, the reaction and sensing performances may be limited considering time scales and sensitivity.

An alternate solution to continuous fluid flow is local mixing of the liquid layer over the sensing surface. Mixing at the microfluidic level is a well known challenging issue since sub-millimetre dimensions, low Reynolds number usually yields laminar flows [18, 19]. Some works propose to induce an active mixing by an additional energy source plugged into the system to create flow instabilities. For example, ultrasonic mixers using stationary wave patterns or surface acoustic waves (SAW) were developed in order to decrease the mixing time and to improve the homogeneity of continuous-flow mixtures [20]. Some micro-devices using microchannels even permit to generate micro-drops of reagents and to coalesce them in a carrier continuous phase [21].

Furthermore, an alternative approach to continuous delivery microfluidic systems is the handling of discrete droplets. The electrowetting-based linear-array droplet mixer, for example, proves that microdroplets can be transported, merged and actively mixed using an electrostatic field [22]. Acoustic field can also be used for that purpose; several examples have been presented using, for the most part, high frequency vibrations such as SAW devices [23]. Pioneer work proves the feasibility of a system composed of a droplet based SPR system coupled to a Surface Acoustic Wave (SAW) microfluidic platform [24]. This opened the door to A. Renaudin and his co-workers to experiment with a device incorporating SPR sensing and a SAW actuation onto a common substrate [25] instead of two independent systems thought of by Galopin [24]. However, they observed that SAW action causes a parasitic SPR

response due to a thermal effect, in addition to the improved surface coverage during the antibody immobilization reaction.

In this paper, we propose a fully acoustic solution combining a Love-wave sensor and a low frequency vibrating mixer in the aim of a real-time monitoring, independent of the SPR system, of biological reactions while they are excited by an active mixing. Within this framework, we wish to assess that mixing increases antibodies (Ab) transfer to a sensing area surface, increases the reaction kinetics by removing the dependency with the protein diffusion coefficient in a liquid, while inducing minimum disturbance to the sensing capability of the Love mode transducer thanks to its low thermal coefficient and differential measurement strategy. We believe that this approach will be the entrance to a real time detection of the binding effect in a spotting mode which still until now considered as a black box.

In the first section, we describe our sensor and mixing system, detailing their structural and operational features and the experimental preparation. We then report on our experimental results on the acoustically stimulated adsorption. We finally propose an analysis of the impact of acoustic mixing on the adsorption process to explain the observed kinetic using the Love-wave sensor.

2. Materials and methods

2.1.Surface acoustic wave sensor

Love-wave devices consist in delay lines built on (AT, Z) cut of quartz for minimizing the temperature drift coefficient around room temperature. The wave guidance is achieved by depositing a 2.5 µm thick silica layer at the top of an AT-cut of quartz, a thickness selected as a trade-off between an acceptable gravimetric sensitivity and a reasonably simple and reproducible sensor fabrication (PECVD silica layer deposition duration). The Love wave is

excited and detected using inter-digital transducers (IDTs) composed of 50 pairs of 4-finger-per-wavelength electrodes made of 200 nm thick aluminium strips deposited by evaporation and patterned using a lift-off process. The grating period is 10 µm, *i.e.* a wavelength close to 40 µm, yielding an operation frequency in the vicinity of 125 MHz. A 3.2 mm long cavity is achieved between the two delay line IDTs, corresponding to the location where biochemical reactions are assumed to take place (the so-called sensing area). This area was covered by successive evaporation and lift-off of 10 nm of titanium and 50 nm of gold. The acoustic aperture is 3.5 mm (about 90 wavelengths). The silica overlays used here as guiding layers are patterned to access the bonding pads [26]. Fig. 1 shows a scheme of the delay line and fig. 2 shows a photo of the dual (differential) delay line. One delay line is dedicated to the sensing operation, whereas the other is used as phase and magnitude reference.

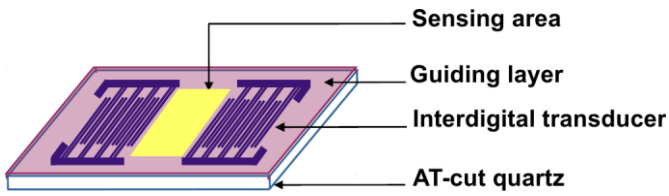

Figure 1: Scheme of the Love-wave based delay line

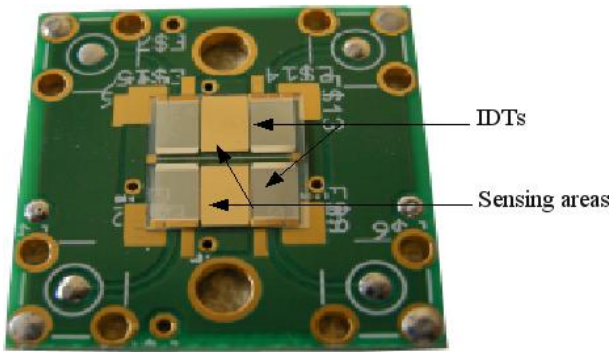

Figure 2: Photo of the dual delay lines device glued on a FR4 epoxy printed circuit (26×26 mm)

Sensor characterization experiments were done with a Rohde & Schwartz network analyzer. Fig. 3 shows the typical response of silica based Love-wave delay lines. The insertion loss is observed near -24 dB.

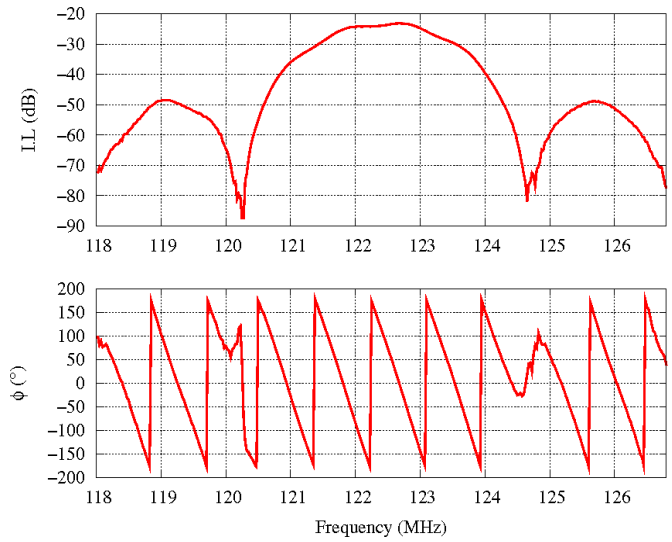

Figure 3: Typical transfer function of delay line exploiting silica guiding overlays (top: insertion loss, bottom: phase)

2.2.Low frequency vibrating mixer

The low frequency vibrating mixer is an acoustic transducer consisting of an active piezoelectric element and a silicon structure. First, membranes 100 µm-thick are structured from a 500 µm-thick silicon wafer by etching in aqueous KOH. A second etching (50 µm) step structures a matrix of 5×5 wells on the top layer in order to receive and easily position 5×5 droplets. After the drying process, we obtain square membrane 12 mm × 12 mm × 50 µm surrounded with a rectangular substrate 25 mm × 30 mm × 450 µm. Then, a massive piezoelectric ceramic 10 mm× 10 mm × 127 µm is centred and then glued to the membrane bottom side using EPOTEK E205 conductive epoxy heated at 80° C [9]. The obtained assembly is then mounted on a Printed Circuit Board (PCB). Electrical connexions are performed using ball bonding technique [27]. The use of a Si structure allows for the choice of the vibration mode. In this study, since our objective is to prove a concept, we will experiment the case of only one droplet instead of 5×5 droplet matrix. Hence, we choose to excite the acoustic mixer at a degenerated vibration mode corresponding to a combination of (1, 3) and (3, 1) modes.

At the resonance frequency, radiation pressure is generated in the droplet, inducing hydrodynamic flow and thus mixing. Eventual particles introduced in the droplet will follow flow lines from the drop centre to the surface. Particle velocity increases with the active element excitation voltage. Since the mixer resonance frequency depends on the droplet volume and this latter changes as function of time due to evaporation phenomena, the resonance frequency changes over time. To ensure that it remains excited during the whole experiment, the transducer will be excited in a sweep mode around the initial resonance frequency 63.9 kHz, corresponding to the resonance frequency of the membrane coupled with a 10 µL droplet. Excitation parameters are given in Table 1.

Table 1: Mixer electrical excitation parameters

Start frequency	63 kHz	Sweep	10 ms
Stop frequency	65 kHz	Hold	0 ms
Signal generator voltage	55 mV	Return	1 ms
Offset	0 mV	Type	Linear
Amplified voltage PP	25V	Interval	1 ms

2.3.Biochemical

The surface functionalization was performed with self assembled monolayer of PolyEthylene Glycol O-(2-mercaptoethyl)-O'-(methoxy)-hexaethylene (mPEG thiol) and O-(2-Carboxiethyl)-O'-(2-mercaptoethyl)-heptaethylene glycol acids (PEG thiol acid) provided by Polypure (Norway). N-hydroxysuccinimide (NHS) and N-(3-dimethylaminopropyl)-N-ethylcarbodiimide (EDC) are used as chemical activating groups and are purchased from Biacore (GE Healthcare, Sweden). Water used in experiments was purified using water purification system (Purelab prima from ELGA) with a resistivity of 18 MΩ.cm. To study the

acoustic excitation influence on the immobilization behavior, we choose to bind the monoclonal antibody A9H12, at 100 µg.mL^{-1} in a 10 mM acetate buffer (pH 5.2), which recognizes specifically Lymphocyte Activation Gene-3 (LAG-3) protein (courteously provided by Immutep SA) (250 nM).

2.4.Sensing area funtionnalization

The SAW sensor was rinsed with ultra pure ethanol and water. This step was followed by an overnight stay in a mixture of mPEG thiol and PEG thiol acids at 100 µM (7/3 by mole). Those components are diluted in 10 mM acetate buffer (pH 4.5). The resulting self-assembled monolayer presents in theory 30% by mol of PEG molecules which bear one carboxyl group. The SAW sensor was rinsed with ultra pure water. Then, the two gold sensing areas are activated using NHS at 50 mM and EDC at 400 mM for half an hour in static mode. After that, the SAW sensor was rinsed with ultra pure water. This procedure prepares the sensing area for the immobilization step. In this way, covalent immobilization of Ab could be accomplished via coupling through their primary amines in passive (without agitation) or active (with agitation) modes. The whole process is summarized in Figure .

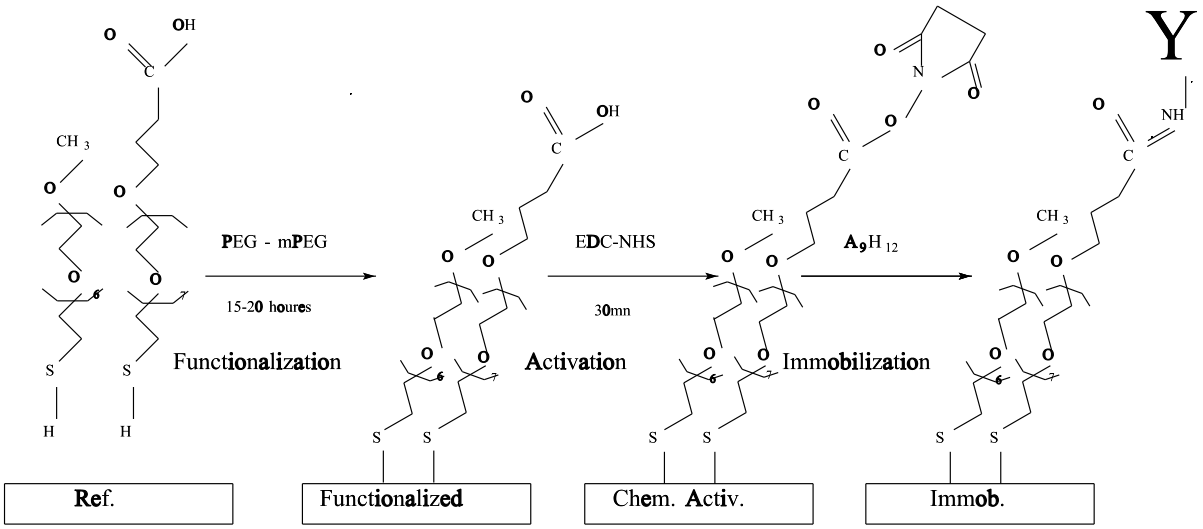

Figure 4: Chemical functionalization steps; Y letter represents the antibody.

3. Results and discussion

We now apply our experimental set-up to study the effect of the acoustic mixing on the biological molecule adsorption to the gold sensing area. For that, we propose two experiments. In the first one, we monitor Ab adsorption on the sensing area in presence and in absence of acoustic mixing. In a second part, we monitor antigenic reaction, in both modes, of a passively immobilized Ab layer.

3.1.Real time detection of Ab binding

We study the influence of acoustic mixing during the immobilization step on microarrays behavior. Binding kinetics parameters identification requires time resolved Ab reaction monitoring. To this aim, we performed a system composed of an acoustic mixer coupled to a Love-wave sensor. The latter is adjusted in x, y and z axis using micrometric positioners in order to precisely sandwich the drop between the Love-wave device sensing area and the mixer membrane (Fig. 5).

a) b)

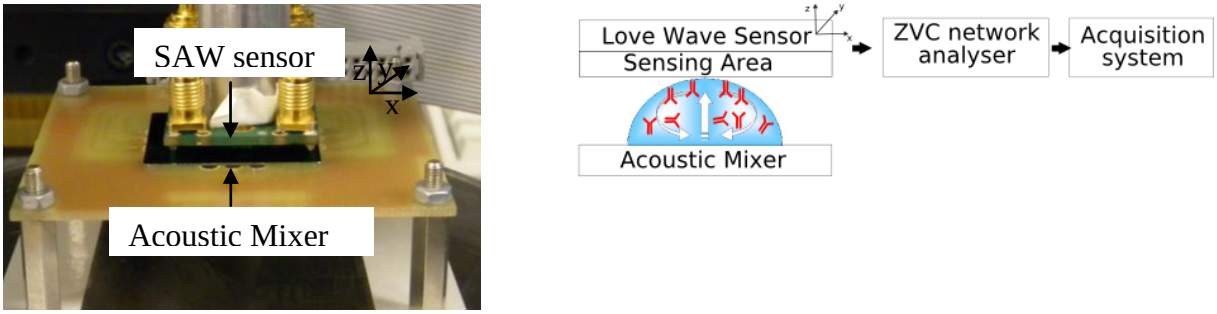

Figure 5: Experimental setup, a) Love-wave sensor adjusted using micrometer positioner in contact with the acoustic mixer through the droplet; b) Functional scheme of the global setup.

The acoustic properties of the acoustic delay line are monitored at a rate of 1 Hz using a GPIB controlled Rohde & Schwartz ZVC network analyzer. The phase and magnitude of the S_{21} transmission coefficient within the band pass frequency range are recorded for post-processing. After its sensing area functionalization, the SAW sensor is rinsed with deionised water several times to clean the sensing area before running the adsorption of antibodies.

As a reference, a 10 µl droplet of acetate buffer 10 mM (pH 4.5), is deposited on the acoustic mixer. This buffer is the same used to dilute antibodies. The Love-wave sensor is then adjusted to precisely put the drop in contact with the sensing area while guaranteeing the absence of contact with the IDTs. Once the contact established, the sensor signal is monitored until a stable baseline at about -27.3 dB/37.7 degrees is reached (Fig. 6, zone 1). After that, due to the lack of an integrated fluidic system allowing for the continuous flow of various reagents, the SAW sensor and the acoustic mixer are separated in order to rapidly clean the mixer and deposit a new droplet containing this time antibodies (Fig. 6, zone 2). As soon as the contact is ensured, a shift of the phase and an insertion loss caused by the second droplet filing indicates the beginning of an Ab-film formation at the sensitive surface (Fig. 6, zone 3). If a washing droplet of buffer solution is put after the classic cleaning step (referred by 4 and 5 on Fig. 6), the acoustic phase signal remains stable testifying of the binding quality.

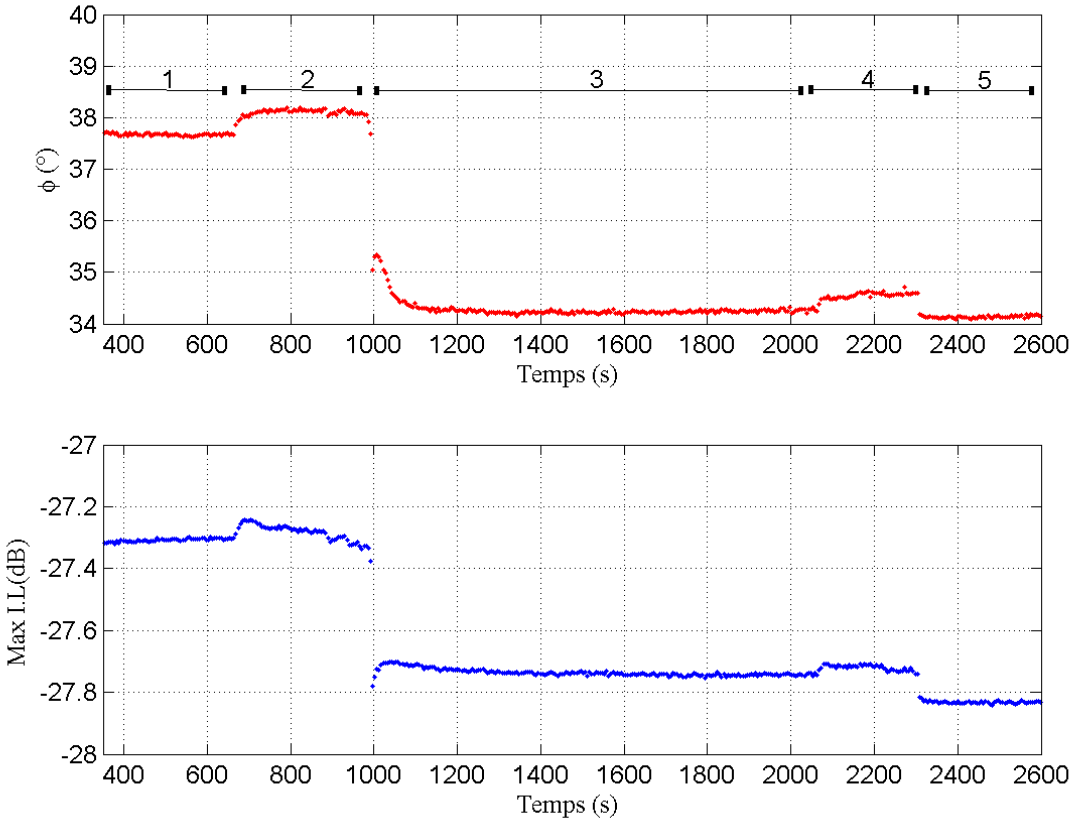

Figure 6: Phase (top) and magnitude (bottom) measurements monitored during Ab immobilization

Since the dual delay lines of the SAW sensor are identical and were submitted to the same chemical functionalization procedure, the two obtained sensing areas are the same. This asset permits a truthful comparison between the active and passive modes of the Ab binding. Fig. 7 exhibits the sensor phase variation in both modes; in presence of acoustic mixing (bottom curves, associated with the largest phase shift) and in absence of active mixing (top curves, associated with a lower phase shift). As we can see in this figure, the mixing increases Ab transfer to the sensing area. In fact, we observe a phase variation of about 8.2 deg±0.3deg in the acoustically activated mode against 3.3deg±0.3deg in passive mode.

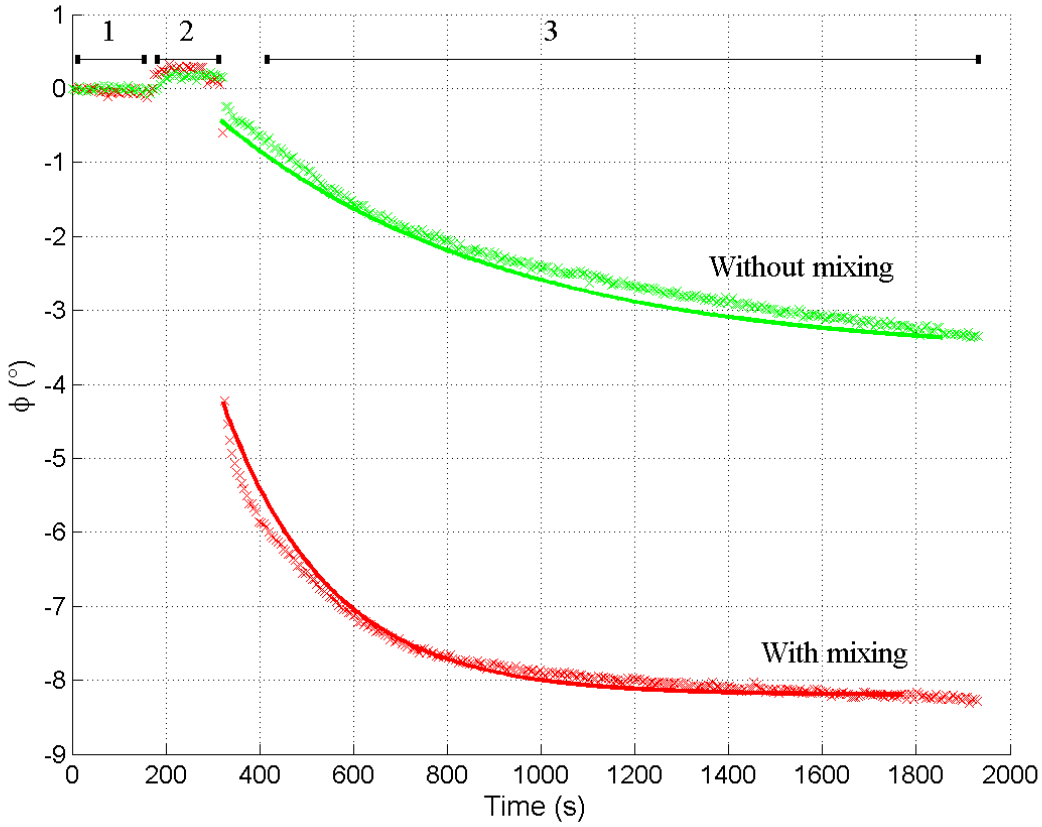

Figure 7: Phase measurements monitored during Ab adsorption for two modes without acoustic mixing (top curves), and with acoustic mixing (bottom curves). The curves are referred to zero at time t=0 to make comparison easier. Crosses are experimental data, solid lines correspond to curve fits following a first order diffusion law.

Consequently, the noted coverage increase thanks to mixing is about 2.5. This value is consistent with the mean gain obtained thanks to acoustic mixing measured using Surface Plasmon Resonance Imaging (SPRi [28]) technique which is about 2.6 [29]: in the experiment reported in this reference, we studied Ab microarrays optical response to antigenic solutions using a SPRi system. Ab microarrays were built in active and passive modes depending whether the transducer is excited or not. Then, they were integrated to the SPRi apparatus in order to characterize their response to antigenic solutions. This experiment showed that antibodies immobilized in active way *via* acoustic mixing answers better to antigenic solutions than passively built microarrays with a mean factor of about 2.6 [29].

3.2. Analysis of acoustic mixing impact on Ab grafting

Beyond the increased coverage, Figure shows a change in reaction kinetics. To highlight this effect, we fit the Ab immobilization curves (Fig. 7, time > 327s) with a classic 1st order law (Equation 1), usually adopted by SPR techniques for kinetics parameters identification [30].

$$\Phi(t) = K(1 - \exp(\frac{t}{\tau})) \qquad \text{Equation 1}$$

Where t is time, τ is time constant and K is a constant depending on concentration.

In the passive case, τ is equal to 582 seconds. This time constant is reduced to 280 seconds by acoustic mixing of the droplet. This proves that acoustic energy makes the reaction faster. Nevertheless, we note that experimental data are not well described with a single exponential manner; especially in the acoustically activated case, where the first two measured points are not taken into account. In this latter case, antibodies immobilization clearly involves two distinct rate processes and will be better described by equation 2.

$$\Phi(t) = K_1[1 - \exp(\frac{t}{\tau_1})] + K_2[1 - \exp(\frac{t}{\tau_2})] \qquad \text{Equation 2}$$

Indeed, in absence of acoustic energy, the biological particles are driven to the biochip surface by diffusion. In the acoustically activated case, we believe that particle drift is due to the combination of the induced displacement force and the natural diffusion except at the vicinity of the biochip where diffusion is dominating.

When only diffusion acts on particles, the governing law is the Fick second law which 1D formulation is given by equation 3 [31]. The x axis is taken perpendicular to the sensor surface and parallel to the concentration gradient.

$$\frac{\delta c}{\delta t} = D\frac{\delta^2 c}{\delta x^2} \qquad \text{Equation 3}$$

If we consider that a quantity of molecules Q is coated as thin film in an infinite liquid (which practically means that the molecule film thickness is negligible with respect to the liquid height), the concentration of molecules along the liquid is given by the following equation [32]:

$$\frac{c(x,t)}{Q} = \frac{1}{2\sqrt{\pi Di.t}} * exp(-\frac{x^2}{4Di.t}) \qquad \text{Equation 4}$$

Where x is the distance in either direction normal to initial solute film, t is time, Di is the diffusion coefficient

The presented model is only valid as first approximation since the particles are initially homogeneously spread in the liquid and not plated in a thin film. In order to properly describe the experiment setup, we suppose that the liquid is an infinite sum of thin molecule films. Each one diffuses form its initial position x_1 in the liquid. Each film contribution is then given by the following relationship:

$$\frac{c(x,t)}{Q} = \frac{1}{2\sqrt{\pi Di.t}} * exp(-\frac{(x-x_1)^2}{4Di.t}) \qquad \text{Equation 5}$$

The molecule quantity Q_m that diffused from the x_1 position and reaches the sensor surface is given by equation 6.

$$Q_m(x_1,t) = \int_{X_{max}}^{\infty} \frac{1}{2\sqrt{\pi Di.t}} * exp(-\frac{(x-x_1)^2}{4Di.t})dx \qquad \text{Equation 6}$$

The total number of molecules that reach the sensor surface, Q_{tot}, at t time is then the sum on the x_1 position of Q_m

$$Q_{tot}(t) = \int_0^{X_{max}} Q_m(x_1,t)dx_1 \qquad \text{Equation 7}$$

This relation best fits the experimental measurement in the passive case for a diffusion coefficient D_i equal to 10^{-9} m^2/s, which is an acceptable value considering that diffusion coefficients of proteins in a liquid varies between $10^{-10}$and 10^{-9} m^2/s [33]. Figure 8 shows a similar behavior of the two curves.

In the acoustically activated case, we consider the liquid as two distinguishable domains. The first one extends form the mixer surface, corresponding to x=0, to an arbitrary position $x_{DD\to D}$. In this phase, the particle movement is governed by both diffusion and acoustic flow lines. The second domain goes from the arbitrary taken interface at $x_{DD\to D}$ to the SAW sensor surface, corresponding to $x=X_{max}$. To analytically limit the displacement force influence to the first domain, we consider the function given by the following system

$$0.5 * erfc(10^5.(x_1 - x_{DD\to D})) = \begin{cases} 1 & if \;\; x < x_{DD\to D} \\ 0 & if \;\; x > x_{DD\to D} \end{cases}$$ Equation 8

where erfc is the complementary error function.

The considered solution of the Fick second law is consequently modified by a mean velocity <v> testifying of the prensence of a displacement force. This magnitude is taken equal to 1 mm/s which is an experimentally determined value (data not shown).

$$\frac{c(x,t)}{Q} = \frac{1}{2\sqrt{\pi Di.t}} * exp(-\frac{(x - x_1 - < v > * t * 0.5 * erfc(10^5.(x_1 - x_{DD\to D})))^2}{4Di.t})$$

Equation 9

For an $x_{DD\to D}$ equal to 0.7 mm, the expression, given by equation 10, shows a similar behavior to the experimental data in the active case.

$$\frac{c(x,t)}{Q} = \int_0^{X_{max}} \int_{X_{max}}^{\infty} \frac{1}{2\sqrt{\pi Di.t}} * exp(-\frac{(x - x_1 - < v > * t * 0.5 * erfc(10^5.(x_1 - x_{DD\to D})))^2}{4Di.t}) dx dx_1$$

Equation 10

(a) (b)

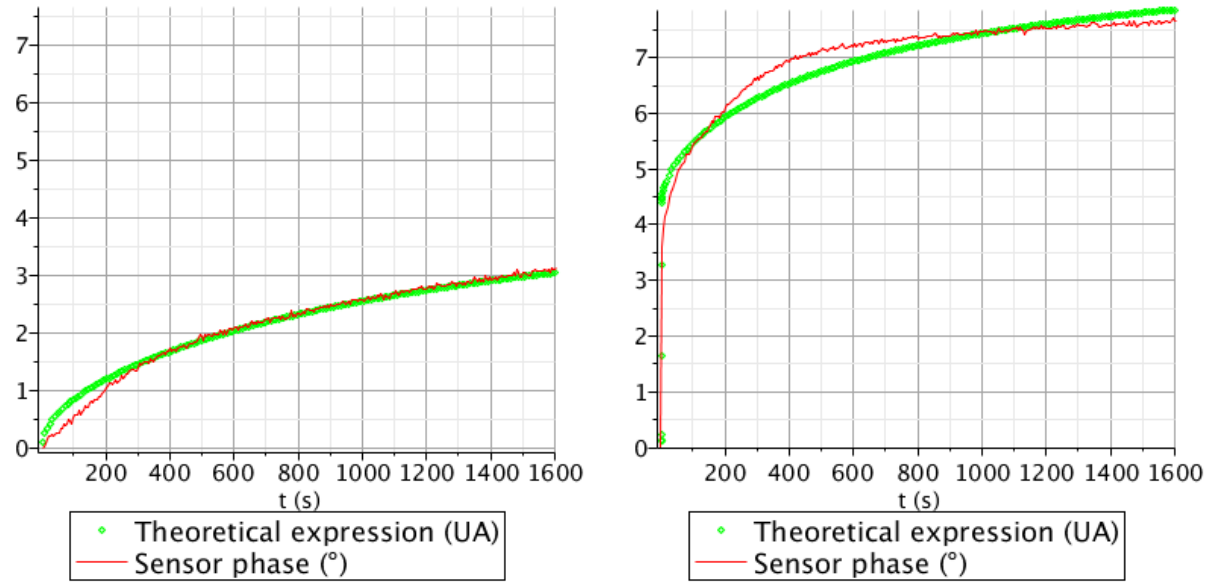

Figure 8: Comparison of normalized phase measurements monitored during Ab adsorption (thin solid lines) with theoretical laws (thick solid lines) in two modes: without acoustic mixing (a), with acoustic mixing (b).

In both passive and active cases, the magnitude of the theoretical expression is not significant, since we focus on the diffusion coefficient identification by using the normalized adsorption curves. Especially, the correspondence of theoretical and experimental time constants as illustrated by Figure 8 testifies of the correctness of our approach. Nevertheless, the presented equations are a 1D formulation of the real problem in order to make calculation easier. A 3D formulation would better approach experimental data.

The immobilized quantity over the sensing area is deduced from the combination of two equations. The phase-frequency slope is given by the acoustic wave velocity, considering that one wavelength propagation is equal to a phase rotation of 360 deg, thus

$$\frac{\Delta\phi}{\Delta f} = \frac{360.L}{V} = 3.7*10^{-4} \quad (^{deg}/_{Hz}) \qquad \text{Equation 1}$$

where V= 5000 m.s^{-1}, is the phase velocity and L= 5.23 mm, is the centre-to-centre distance between the IDTs.

On the other hand, the mass sensitivity S for acoustic wave sensors is defined as the incremental frequency change occurring in response to an incremental change in mass per unit of area A on the surface of the device as follows:

$$S=\frac{\Delta f}{f_0}\frac{A}{\Delta m}\ (cm^2/g)$$ Equation 2

Where Δm is the uniformly distributed mass per unit of area added to the surface of the device, f_0 (125 MHz) is the unperturbed resonance frequency of the device and Δf is the change in the operational frequency due to mass loading effect, the gravimetric sensitivity was measured in liquid phase and is equal, for these sensors, to 250 cm²/g [34]. It follows from equations 2 and 3, the expression of the surface density (Equation 4).

$$\frac{\Delta m}{A}=\frac{\Delta\Phi}{f_0 \cdot S\ *3.7*10^{-4}}\ \left(g/cm^2\right)$$ Equation 3

The phase shift corresponding to active and passive modes are respectively 8.2deg±0.3deg and 3.3deg±0.3deg (Fig. 7) and the absorbed mass are respectively 713 ng/cm² and 290 ng/cm², using equation 3.

3.3. Experimental assessment of the acoustic mixing influence on Ab-Ag reaction

Since we have observed an important improvement of the antibody immobilization thanks to acoustic mixing, we have investigated the influence of this energy on the immobilized layer response to antigenic solution. To do that, we have passively Ab immobilized the two sensing areas of the sensor. In fact, an Ab containing droplet was deposited on each sensing area during 30 mn. After that, the sensor was incubated in ethanolamine (1 M) to target free NHS entities in order to deactivate the sensing areas. It is then rinsed with ultrapure water. Our previous measurements allow as estimating the Ab surface density to be about 300 ng/cm² (see prg. 2.1). The sensor is now prepared to begin

acquisition (Fig. 9). We proceed, as in the Ab immobilization monitoring, by taking, first, a baseline reference (zone 1). In this case, the reference is the antigen buffer PBS. After the cleaning step (referred to as 2 in Fig. 9), a 10 µL droplet of antigenic solution is deposited on the acoustic mixer membrane. Since the contact is ensured the Ab-Ag reaction begins (Fig. 9, zone 3). We have realized this experiment in both active and passive modes. Without acoustic mixing during antigenic reaction, the phase shifts with 3.6 deg±0.3deg, which corresponds to an Ag surface density of 311 ng/cm², which is consistent with previously established SPR experiments (data not shown) exhibiting saturating levels at a molar ratio of 1/1 (when 50% of Fab sites are occupied) for this Ab/Ag couple. This means that the expected Ag surface density is equal to the one of the Ab layer, 300 ng/cm². The antigenic response in the acoustically excited case induces a phase shift of about 4.5deg±0.3deg, corresponding to 389 ng/cm² surface density. The global increase compared to the passive case is about 20%. This means that acoustic mixing permitted antigens to find away the classically unbound Fab sites.

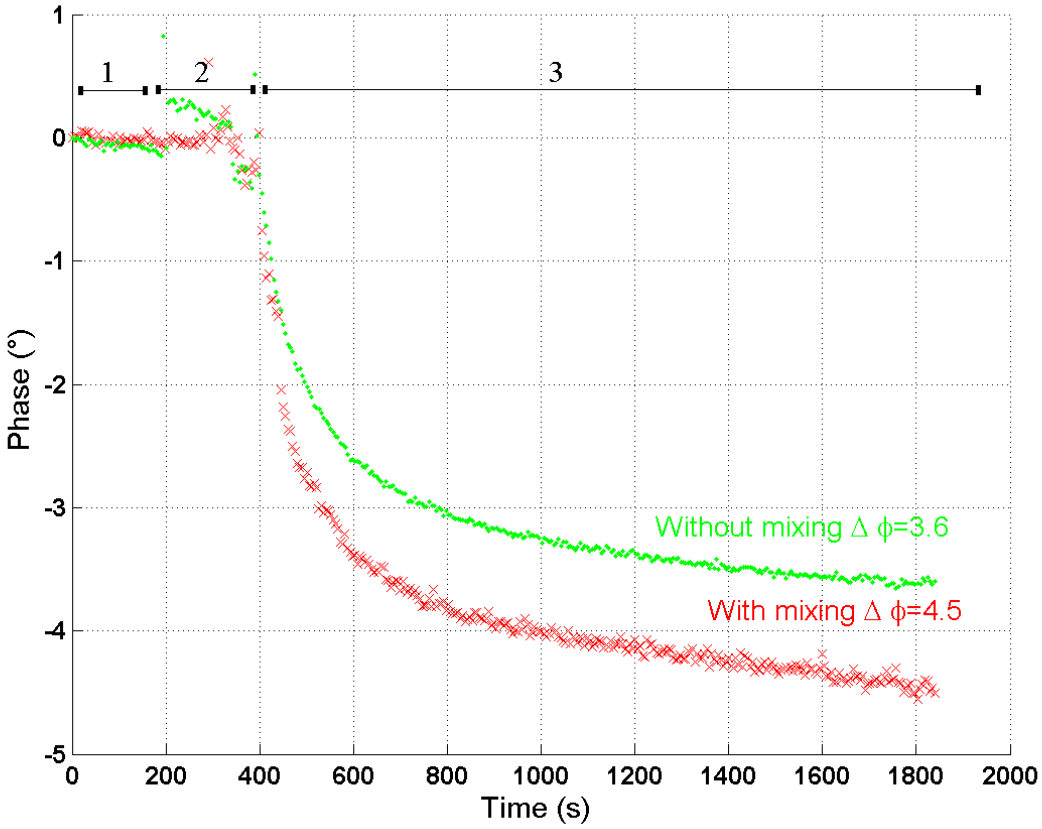

Figure 9: Phase measurements monitored of Ab layer response to antigenic solution for two modes without acoustic mixing (circles, top curve), with acoustic mixing (crosses, bottom curve). The curves are referred to zero at time 0 to make comparison easier.

Conclusions

We propose a Love wave sensor whose phase shifts as function of the immobilized Ab quantity, combined with an active acoustic mixing device. We demonstrate its use during the immobilization step for improved coverage while keeping the thermal effect below detectable limits.

We have assessed that mixing at the droplet level increases antibodies (Ab) transfer to a sensing area surface, increases the reaction kinetics by removing the dependency with the protein diffusion coefficient in a liquid, while inducing minimum disturbance to the sensing capability of the Love mode. We have tested the global system composed of the acoustic mixer coupled to the SAW sensor. In this way, we proved that the Ab density on the sensing surface is improved by acoustic mixing with a gain factor of about 2.5. Beyond the asymptotic transfer rate, the time dependent kinetic modelling yields a protein diffusion coefficient consistent with the literature in the case of the static drop, and an increased transfer rate dependent on the fluid velocity in the case of acoustic mixing. Typical fluid velocities in the mm/s range included in Fick diffusion law yield best fit of the experimental data.

This experiment showed also an improvement of the captured Ag density of 20 % compared to the passive antigenic interaction.

Acknowledgment

The authors would like to thank Benoît Simon and Alain Rouleau for their assistance in biological solution preparation. We also thank Dr. Frédéric Triebel (from Immutep SA) for

providing A9H12/LAG-3 model and the clean room and technology platform MIMENTO (Besançon, France).

Bibliography

[1] Gizeli, E., and Lowe, C.R., "Biomolecular Sensors", 2002.

[2] Gronewold, T.M.A., "Surface acoustic wave sensors in the bioanalytical field: Recent trends and challenges", Anal. Chim. Acta., 603 (2), 119-128, 2007.

[3] Jakoby, B., and Vellekoop, M., "Viscosity sensing using a love-wave device", Sens. and Act. (A), 68, 275–281, 1998.

[4] El Fissi, L.; Friedt, J-M.; Luzet, V.; Cherioux, F.; Martin, G.; Ballandras, S., "A Love-Wave sensor for direct detection of biofunctionalized nanoparticles", IEEE Frequency Control Symposium, 861 – 865, 2009.

[5] El Fissi, L., Friedt, J.-M., Chérioux, F., Ballandras, S., "Amine functionalized SU-8 layer guiding Love mode surface acoustic wave", Sens. and Act. (B). 144, 23-26. 2010.

[6] Modin, C., Stranne, A.-L., Foss, M., Duch, M., Justesen, J., Chevallier, J., Andersen, L. K., Hemmersam, A. G., Pedersen, F. S., and Besenbacher, F., "QCM-D studies of attachment and differential spreading of preosteoblastic cells on Ta and Cr surfaces". Biomaterials, 27, 1346-1354, 2006.

[7] Kößlinger, C., Uttenthaler, E., Drost, S., Aberl, F., Wolf, H., Brink, G., Stanglmaier, A., and Sackmann, E., 1995 "Comparison of the QCM and the SPR method for surface studies and immunological applications". Sens. Act. (B), 24, 107–112.

[8] Malmström, J., Agheli, H., Kingshott, P., and Sutherland, D.S., "Viscoelastic modelling of highly hydrated laminin layers at homogeneous and nanostructured surfaces: Quantification of protein layer properties using QCM-D and SPR", Langmuir, 23(19), 9760-9768, 2007.

[9] Wilczewski, M., Van der Heyden, A., Renaudet, O., Dumy, P., Coche-Guerente, L., and Labbe, P., "Promotion of sugar-lectin recognition through the multiple sugar presentation offered by regioselectively addressable functionalized templates (RAFT): a QCM-D and SPR study", Org. Biomol. Chem., 6 (6), 1114-1122, 2008.

[10] Bender, F., Roach, P., Tsortos, A., Papadakis, G., Newton, M. I., McHale, G., and Gizeli, E., "Development of a combined surface plasmon resonance/surface acoustic wave device for the characterization of biomolecules", Meas. Sci. Technol. 20 (12), 124011, 2009.

[11] Mangeat, T., Berthier, A., Caille, C. E., Perrin, M., Boireau, W., Pieralli, C., and Wacogne, B., "Gold/Silica biochips: Applications to Surface Plasmon Resonance and fluorescence quenching", Laser physics, 19 (2), 252-58, 2009.

[12] K. Mitsakakis, A. Tserepi, E. Gizeli, "SAW device integrated with microfluidics for array-type biosensing", Microelectronic Engineering 86, 1416–1418, 2009.

[13] K. Mitsakakis, A. Tserepi, and E. Gizeli, "Integration of Microfluidics With a Love Wave Sensor for the Fabrication of a Multisample Analytical Microdevic", J. of Microelectromechanical Systems, 17 (4), 1010-1019, 2008

[14] G. Ohlsson, P. Axelsson, J. Henry, S. Petronis, S. Svedhem, B. Kasemo, "A miniaturized flow reaction chamber for use in combination with QCM-D sensing", Microfluid Nanofluid (2010) 9:705–716

[15] Liedberg, B., Nylander, C., Lundstrom, I., " Biosensing with surface plasmon resonance — how it all started". Biosens. Bioelectron., 10, 1–4,1995.

[16] Boireau, W., Rouleau, A., Lucchi, G., Ducoroy, P., "Revisited BIA-MS combination: Entire "on-a-chip" processing leading to the proteins identification at low femtomole to sub-femtomole levels", Biosensors Bioelectronics, 24, 1121–1127, 2009.

[17] Karlsson, R., Roos, H., Fagerstam, L., Persson, B., "Kinetic and Concentration Analysis Using BIA Technology", Methods 6, 99–110, 1994.

[18] Tabeling, P., "Introduction to Microfluidics", Oxford University, 2005.

[19] Squires T.M., and Quake S.R., "Microfluidics: Fluid physics at the nanoliter scale", Rev. Mod. Phys., 7, 977-1026, 2005.

[20] Tan, M. K., Friend J. R., Yeo, L. Y., "Surface acoustic wave driven microchannel flow", 16th Australian Fluid Mechanics Conference, 790–793, 2007 .

[21] Song, H., Bringer, M. R., Tice, J. D. , Gerdts, C. J., and Ismagilov, R. F., "Experimental test of scaling of mixing by chaotic advection in droplets moving through microfluidic channels", Applied Physics Letters, 83, 4664–4666, 2003.

[22] Paik, P., Pamula, V. K., Pollack, M. G., and Fair, R. B., "Electrowetting-based droplet mixers for microfluidic systems," Lab Chip, 3, 28-33, 2003.

[23] Lee, A., Lemoff, A., Miles, R., "MagnetoHydroDynamic (MHD) driven droplet mixer", patent WO 03/078040, 2003.

[24] Galopin, E., Beaugeois, M., Pinchemel, B., Camart, J.-C., Bouazaoui, M., Thomy, V., "SPR biosensing coupled to a digital microfluidic microstreaming system", Biosens. Bioelectron., 23, 746–750, 2007.

[25] Renaudin, A., Chabot, V., Grondin, E., Aimez, V., Charrette, P. G., "Integrated active mixing and biosensing using surface acoustic waves (SAW) and surface plasmon resonance (SPR) on a common substrate", Lab Chip, 10, 111–115, 2010.

[26] El Fissi, L., "Detection and measurement of nanoparticles for the sensors applications in liquid medium", PhD, University of Franche-Comte in Besançon (France), 2009 [in French].

[27] Kardous, F., Yahiaoui, R., Manceau, J.-F., "Performing microdroplets mixing using an acoustic transducer with low vibration frequencies", IEEE International Ultrasonics Symposium Proceedings, 2533-2536, 2009.

[28] B.P. Corgier, S. Bellon, M. Anger-Leroy, L.J. Blum, C.A. Marquette, "Protein-Diazonium Adduct Direct Electrografting onto SPRi-Biochip", Langmuir, 25(16), 9619–9623 (2009)

[29] Kardous, F., Rouleau, A., Simon, B., Yahiaoui, R., Manceau, J.-F., Boireau, W., "Improving immunosensor performances using an acoustic mixer on droplet microarray", Biosens. Bioelectron., 26 (4), 1666-1671, 2010.

[30] Maillart, E., "Développement d'un système optique d'imagerie en résonance de plasmons de surface pour l'analyse simultanée de multiples interactions biomoléculaires en temps réel", PhD, University of Paris XI (France), 2004 [in French].

[31] Crank, J., "The mathematics of diffusion", Oxford University Press, 1956.

[32] Fischer, H. B., List, J. E., Koh, C. R., Imberger, J., and Brooks., N. H., "Mixing in Inland and Coastal Waters", Academic Press (1979).

[33] Brune, D., and Kim, S., "Predicting protein diffusion coefficients". PNAS, 90, 3835-3839, 1993.

[34] Friedt, J.-M., Choi, K.H., Frederix, F., Campitelli, A., "Simultaneous Atomic Force Microscope and Quartz Crystal Microbalance Measurements: Methodology Validation using Electrodeposition", J. Electrochem. Soc., 150, 229-234, 2003.

Biographies

Faten Kardous was born in Tunis (Tunisia) in 1983. She received her engineering degree from the ENSEEHIT engineering school in Toulouse (France) in 2007. In the same year, she obtained her master of science from the Polytechnic National Institute (INP) of Toulouse. She is currently completing her Ph.D. study at the University of Franche-Comte in Besancon (France). Her current research interests are investigating acoustic interaction with fluids, developing acoustic transducers and microfluidic devices for lab-on-chip applications devoted to biology.

Lamia El-Fissi was born in Casablanca (Morocco) in 1980. She received her Ph.D. from University of Franche-Comte in Besancon (France) in 2009. Her current research interests are design, fabrication and development of SAW sensors and microfluidic devices for applications of lab-on-chip devoted to biology.

Jean-Michel Friedt obtained his PhD from University of Franche-Comte in Besancon (France) in 2000. Following a 3 years position as a postdoctoral fellow with the Biosensors group in IMEC (Leuven, Belgium), he joined the team of S. Ballandras at the FEMTO-ST institute in Besancon (France) and is currently employed by the company SENSeOR. His interests include direct detection biosensors using optical and acoustic

methods, scanning probe microscopy, and especially the combination of these techniques for multiparametric data analysis.

François BASTIEN was born in 1941, is professor emeritus at University of Franche-Comté (Besançon, France). He works in many fields including plasma physics, piezoelectricity, acoustics, sensors, actuators and micro-system. His current research is mainly on Lamb wave sensors.

Wilfrid Boireau joined the CNRS in 2001 after a post doctoral position in the Center of Molecular Genetics (CGM, Gif/Yvette, France). He obtained his Ph.D degree in enzymatic engineering from the University of Technology of Compiègne (UTC, France) in 1999. His current researches are based at the interface of bio-engineering, micro-technologies and nanostructured materials for the development of new generation of sensors and analytical platforms in the field of clinical proteomic in the Micro Nano Sciences & Systems department (MN2S) of FEMTO-ST Institute. Moreover, he co-founds the "Clinical - Innovation Proteomic Platform" (CLIPP) in 2008 and is the head director of CLIPP since 2010.

Réda Yahiaoui received the M.S. degree in Electronics Sensors and Integrated Circuits - Option Microwaves and Fast Electronic in 1998. He obtained his PhD degree in engineering science in 2002, from the Paris-XI University in Orsay (France). He worked as Research Engineer in Electronics and project management in UAV development until 2005. Actually, he works as assistant professor in the Micro Nano Sciences & Systems department (MN2S) of FEMTO-ST Institute in Besancon (France). His main interests are in fluidic MEMS design, fabrication and modelling.

Jean-François Manceau was born in 1968, he received the aggregation degree in electrical engineering from the Ecole Normale Supérieure de Cachan in 1991 followed by the DEA (Master) degree in 1992. He moved to Besançon (France) to work on ultrasonic micro-actuators and obtained the Ph.D. degree from University of Franche-Comté in 1996. He was Assistant Professor from 1996 to 2004. At the present time, he is Professor at the University of Franche-Comté. His current researches concerns acoustic interactions with fluids applied to sensors or actuators and design of micro-actuators for microfluidic applications within the Micro Nano Sciences & Systems (MN2S) Department of FEMTO-ST Institute.

Sylvain Ballandras joined the CNRS in 1991, after his Ph.D. in Engineering Sciences from the University de Franche-Comté. Until 1995, he has been working on SAW devices, but he was also involved in microtechnologies. He has initiated the development of a finite element analysis package devoted to acoustic transducers and also new researches on miniaturized transducers. During 1997, he achieved a 1 year industrial training project in SAW industry. In October 2003, he was promoted Research Director at the CNRS. In 2008, his group joined the Time-Frequency Department and moved to the national engineering school ENSMM. Its present scientific developments concern fundamentals in acoustics and guided propagation as well as technologies dedicated to acousto-electronic devices and systems, focused on sources, filters and sensors. Sylvain Ballandras also benefits from the 25.2 agreement of the French research rules to join the head staff of SENSeOR since the end of 2008.